Physics of Plasmas

Spontaneous multi-keV electron generation in a low-RF-power axisymmetric mirror machine

Cite as: Phys. Plasmas **26**, 060701 (2019); https://doi.org/10.1063/1.5093905
Submitted: 25 February 2019 . Accepted: 21 May 2019 . Published Online: 07 June 2019

C. Swanson, and S. A. Cohen

Physics of Plasmas LETTER scitation.org/journal/php

Spontaneous multi-keV electron generation in a low-RF-power axisymmetric mirror machine

Cite as: Phys. Plasmas **26**, 060701 (2019); doi: 10.1063/1.5093905
Submitted: 25 February 2019 · Accepted: 21 May 2019 ·
Published Online: 7 June 2019

C. Swanson[1,a)] and S. A. Cohen[2]

AFFILIATIONS

[1]Princeton Satellite Systems, Plainsboro, New Jersey 08536, USA
[2]Princeton Plasma Physics Laboratory, Princeton University, Princeton, New Jersey 08543, USA

[a)]Electronic mail: charles.swanson@psatellite.com

ABSTRACT

X-ray emission shows the existence of multikilo-electron-volt electrons in low-temperature, low-power, capacitively coupled RF-heated magnetic-mirror plasmas that also contain a warm (300 eV) minority electron population. Though these warm electrons are initially passing particles, we suggest that collisionless scattering—μ nonconservation in the static vacuum field—is responsible for a minority of them to persist in the mirror cell for thousands of transits during which time a fraction is energized to a characteristic temperature of 3 keV, with some electrons reaching energies above 30 keV. A heuristic model of the heating by a Fermi-accelerationlike mechanism is presented, with μ nonconservation in the static vacuum field as an essential feature.

Low temperature plasmas, formed at low gas pressure by a low-power radio-frequency (RF) method, are used to study basic plasma phenomena, e.g., wave propagation and absorption, plasma heating, plasma transport, solar flares, magnetic reconnection, parametric instabilities, turbulence, etc.,[1–3] and for numerous practical applications including plasma processing and rocket propulsion.[4,5] In these studies and applications, the plasma is assumed to be a cool near-Maxwellian and is investigated with diagnostics whose response and sensitivity are tailored to the low plasma-temperature regime, $T_e < 10$ eV, though some diagnostics may have an energy range extending to near 100 eV.

In a previous paper,[6] we showed that this assumption is not always justified. We reported the discovery of a minority population of warm (300 eV) electrons created in a low-pressure, low-power, low-temperature, RF-formed plasma. This population was invisible to Langmuir probes; the electron saturation current of this population was far smaller than the ion saturation current of the bulk. In this paper, we show that another minority population develops and violates the cool Maxwellian assumption ($T_e < 10$ eV) still more strongly, becoming heated to a characteristic temperature of 3 keV. We explain this by invoking a novel multidimensional Fermi-type 2nd-order heating process. The presence of a kilo-electron-volt minority population can strongly affect the properties of these low-temperature basic plasma experiments and processing reactors.

Other authors[7–11] have described the production of higher density (to 10^{13}–10^{15} cm^{-3}) hot electron distributions when externally applied high-power (10 kW–10 GW) pulsed electron beams pass through cool plasmas. The electron heating in these experiments is attributed to electrostatic turbulence along the entire beam, essentially along the entire plasma column. The oscillating electrostatic potential that develops is on the order of the beam energy, ca. 10–100 kV.

Multikilo-electron-volt electrons have also been generated in mirror machines by 1- and 2-frequency electron cyclotron resonance (ECR) heating,[12–14] a process that improves confinement. The second frequency is typically considered to be required in order to eliminate adiabatic boundaries to electron heating; our heuristic model replaces this second frequency with the natural nonadiabatic mobility of μ in the static vacuum field.

Herein, we report on the spontaneous development of a hot (3 keV) electron minority population in the center cell (CC) of a low-power, sub-ECR, RF-formed mirror-machine plasmas with no high-power electron beam injected. In this experiment, a centimeter-scale, low current, ca. 500 eV, electron beam spontaneously forms near one mirror coil. This beam generates weak, localized, axial electrostatic field oscillations through two-stream instability. Based on the background gas density, electric and magnetic field characteristics, and power dependences of the hot-electron component's density and temperature, we attribute the hot electron generation to a combination of several effects, primarily μ-nonconservation and interaction with the electrostatic oscillation at the electron-beam end of the CC. These contribute to a multidimensional Fermilike longitudinal electron heating

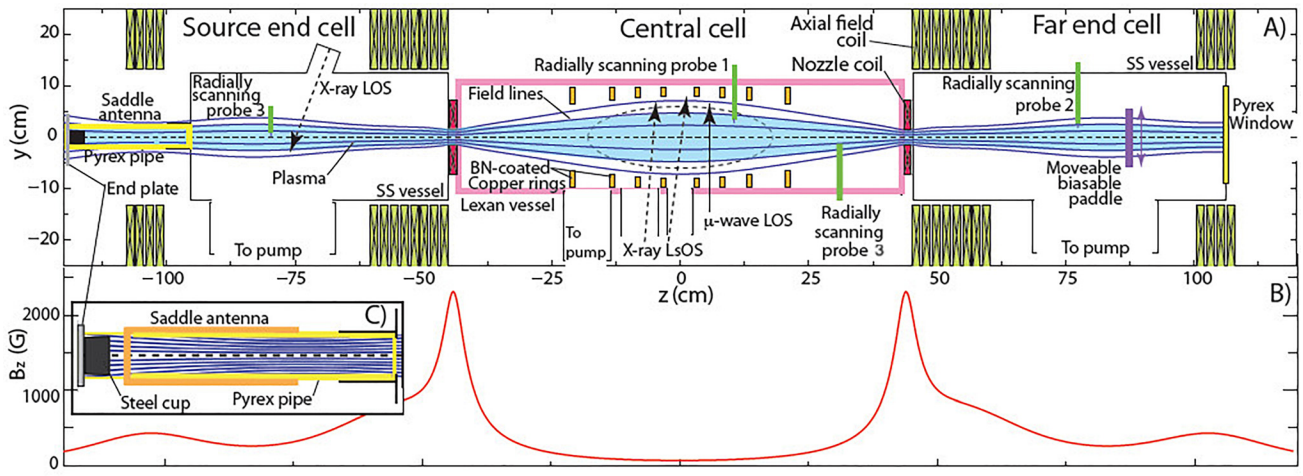

FIG. 1. Schematic of the apparatus (top); typical axial field strength (bottom); details of the RF antenna region (bottom inset). The primary plasma (light blue) is formed via RF heating and secondary electron emission in the antenna region of the source end cell[6] and flows into the central cell and far end cell. Three SDD lines-of-sight (LsOS) are shown (dashed arrows).

that is ordinarily assumed to be unsuitable due to heating-induced particle loss and adiabatic barriers to electron energization.

A schematic representation of the apparatus is shown in Fig. 1. It is the same apparatus as used for the PFRC-II experiments,[15] herein run solely as a low-power magnetic mirror. In these experiments, typical central-cell midplane, i.e., $z = 0$, magnetic field strengths are 50–250 G with a controllable mirror ratio of 10–40. The gas fill in the CC is typically 0.1–0.2 mTorr of H_2 gas. The typical forward power is 300 W. At the neutral density in these experiments, 1 keV electrons have a mean-free path in the CC, based on the total collision cross section, of $\sim 10^4$ cm.

Because of our interest in higher temperature plasmas, we have been using an electron energy diagnostic, an energy-resolved (pulse-height), rapid-response, silicon-drift X-ray detector (SDD),[16] which is sensitive in the range of 0.2–100 keV. The SDD has an energy resolution, $\Delta E/E$, where E is the X-ray energy, of 0.03–0.1. The Electron Energy Distribution Function (EEDF) can be extracted from the raw data by a spectral inversion process and an absolute density calibration process developed for this purpose.[17]

Based on information from this detector when viewing the source end cell (SEC), we have previously reported on a population of warm ($T_e \sim 300$ eV) electrons in the plasma when low-power RF is applied using an external, capacitively coupled antenna. The cause of these electrons has been shown to be secondary electron emission from antenna-proximate RF-self-biased surfaces in contact with the plasma.[6]

Hot electrons (3 keV, as opposed to warm electrons, 300 eV) are observed when the SDD views across the CC near its midplane. They are observed only when the CC pressure is low, 0.1–0.2 mTorr, and not above 0.3 mTorr in the CC.

Figure 2 shows an X-ray spectrum measured in the CC and its derived EEDF. (SEC X-ray spectra were simultaneously monitored and showed a 1% minority population with $T_e \sim 300$ eV.) The CC spectrum between 3 and 18 keV is well characterized by $T_e = 2.55$ keV (hot component); below 2 keV, $T_e = 500$ eV (warm component) is found, about twice that in the SEC under these conditions. Also present are weak spectral lines, mainly of N, Ar, and Fe, the latter presumably due to the plasma impact on a steel surface near the antenna.

Radial profiles of the X-ray signals with Ar and Ne fill gases confirmed that wall fluorescence was not the cause of the X-rays.[6]

The bulk electron T_e and n_e in the CC were not typically measured concurrently with the warm and hot electron parameters, but when measured were $T_e \sim 5$ eV, $n_e \sim 10^{10} - 10^{11}/\text{cm}^3$.

The dependence of the line-averaged, spectrally inverted, Maxwellian-fit hot T_e and hot n_e is shown in Fig. 3 as functions of RF power. Also shown is the normalized peak-to-peak floating potential of 200 ± 20 MHz oscillations, V_{pp}, of a Langmuir probe in the CC near the nozzle coil separating the CC from the Far End Cell (FEC). Hot T_e is seen to rise by a factor of 3 with power as does V_{pp}.

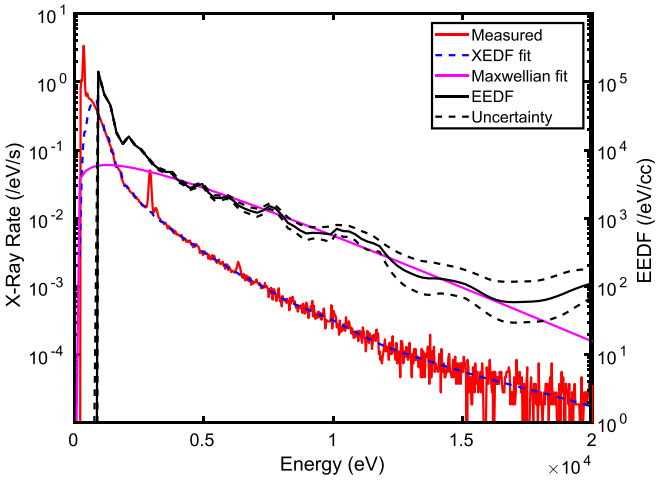

FIG. 2. Raw X-ray data (red); inverted[17] EEDF (black solid); 1σ uncertainty in EEDF (black dashed); Maxwellian EEDF with $T_e = 2.55$ keV and $n_e = 3.2 \times 10^7$/cc (magenta). The raw data show X-rays of energies even out to 30+ keV (not shown).

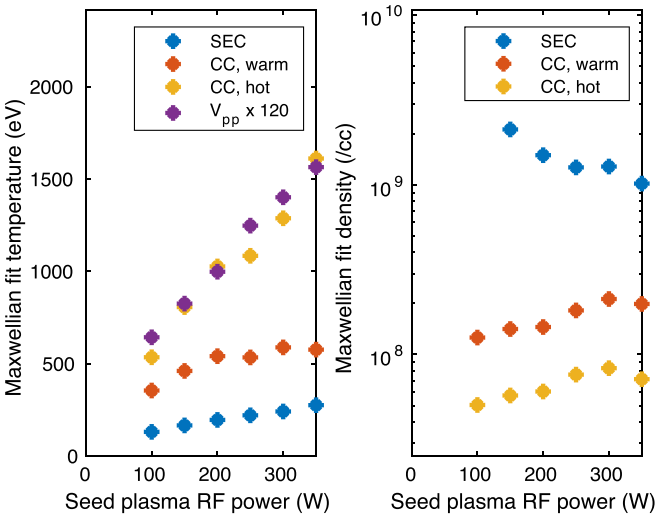

FIG. 3. Minority electron population T_e and n_e derived from X-ray signals and scaled peak-to-peak electrostatic oscillation (V_{pp}) vs the RF forward power. The CC pressure was 0.125 mTorr of H_2 gas. Temperature and density uncertainty result from the fit and are $<10\%$.

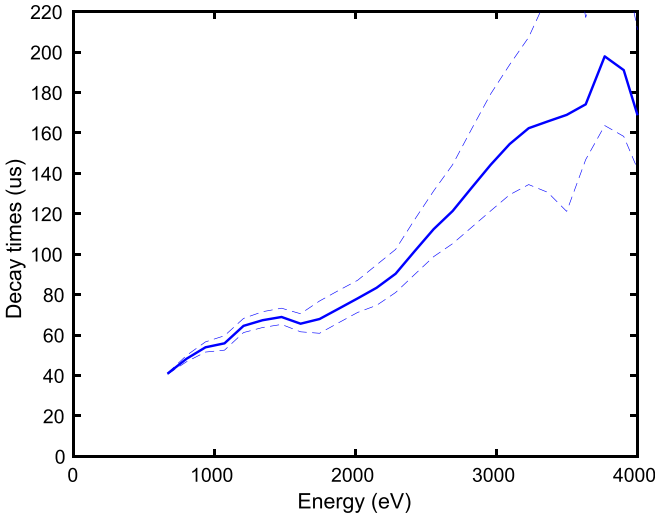

FIG. 4. Decay time of EEDF derived from X-ray spectrum, vs energy (solid line). 1σ uncertainty of decay time (dashed lines).

Autocorrelation and FFT analyses of V_{pp} show a narrow peak at the RF frequency, 19 MHz in this case, and decreasing amplitude narrow peaks at harmonics up to and beyond 200 MHz. The time-averaged Fourier amplitude of the 10th peak is 20 dB below that of the fundamental. 200 MHz is at least a factor of 2.5 below the electron cyclotron resonant (ECR) frequency in the midplane and a factor of 10 below the ECR frequency at the location where V_{pp} is measured. Based on this, we estimate that ECR is of lesser importance to the generation of high energy electrons. In contrast, our heuristic model makes use of the broadly coherent near-200-MHz electrostatic oscillations, which are unrelated to the RF. 200 MHz is near the plasma frequency ω_{pe} of the warm population and much lower than the plasma frequency of the bulk (cold) population. The specific case of two-stream instability in a 3-component bulk, warm, and beam plasma, of which the bulk and beam are in the two-stream beam regime but the warm and beam are in the two-stream Landau regime, does not appear to have been studied in the literature but would appear to have its most unstable mode close to ω_{pe} of the bulk population.[18,19] We do not account for this discrepancy.

By square-wave modulating the RF power, we can determine both the heating and loss-plus-cooling rates for these fast electrons. Figure 4 (solid line) shows the decay time after cessation of the RF for the EEDF signal, using narrow bands of energies. Figure 4 shows the decay time up to 4 keV, as above this, the uncertainty due to the energy-resolution process grows large. Nonenergy-resolved measurements indicate that at least some electrons have decay times longer than 1 ms ($E \gg 8$ keV). The rise time after the initiation of RF power also increases with X-ray energy. These findings indicate a gradual energization and loss mechanism, occurring over thousands of mirror transits.

The dependence on FEC pressure of V_{pp} and the CC and SEC effective temperatures and densities are shown in Fig. 5 and the FEC space potential in Fig. 6. As the pressure is increased, the CC hot T_e and V_{pp} double while warm T_e increases 30% and SEC warm T_e falls 30%. Above p $\sim$ 50 μT, the hot population suddenly disappears simultaneously with the FEC space potential rising to 0 and the FEC endplate (paddle, see Fig. 1) potential (not shown) also rises to zero from its highly negative potential, ca. -1200 V. The (visible-wavelength) brightness and plasma density in the FEC and the heat flux to the paddle also rise dramatically as the gas pressure increases. The paddle potential is a measure of the relative fluxes of fast and bulk electrons. During these experiments, the plasma space potential in the CC and SEC is close to zero. These measurements broadly support the proposed mechanism for electrostatic oscillation generation and electron generation given later in this letter.

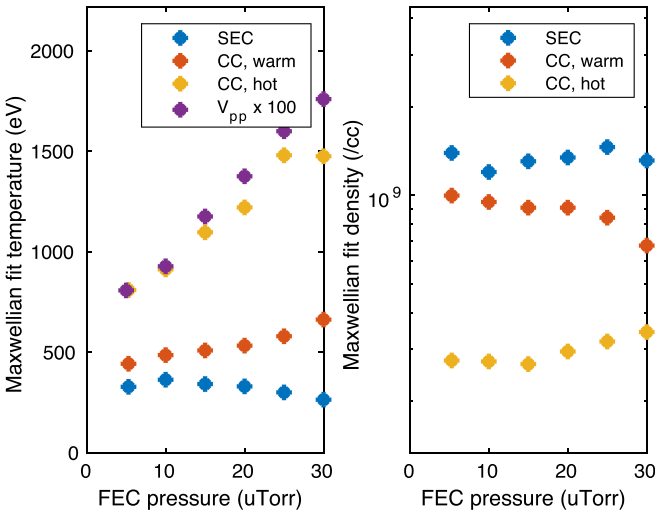

FIG. 5. Minority electron population T_e and n_e derived from X-ray signals and scaled peak-to-peak electrostatic oscillation (V_{pp}) vs FEC gas pressure. The CC pressure was held constant at 0.133 mTorr of H_2 gas.

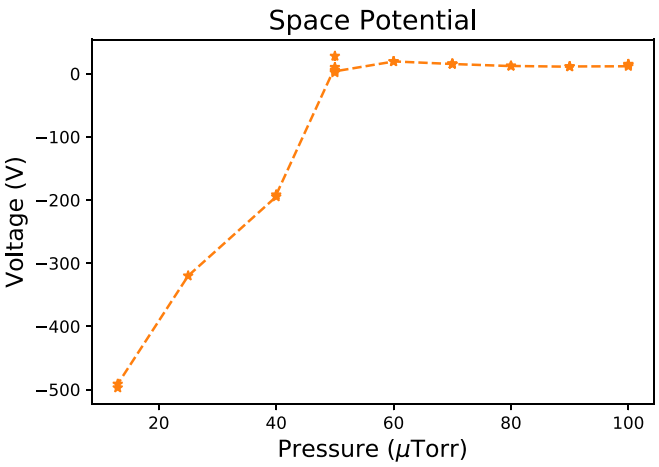

FIG. 6. FEC plasma space potential vs FEC gas pressure.

The average electron kinetic energy is higher at larger radii, see Fig. 7, one of several observations that strongly support the interpretation that μ nonconservation near $z = 0$ is the dominant cause of the required velocity-space randomization needed for particle heating.

The CC hot T_e and maximum electron energy are both far greater than the paddle potential and potentials in the SEC. This shows us that electrostatic confinement is not the cause of the electron confinement or heating.

The 200 MHz electrostatic oscillations noted previously are similar to those seen in other experiments[20] where the plasma expands through a magnetic nozzle, forming a double layer there. Here, we speculate on the source of these oscillations:

There is likely a double-layer structure in the PFRC-II; see Fig. 6. The space potential was measured by a Langmuir probe in the FEC (Radially scanning probe 2 in Fig. 1). It was determined by the inflection point method and checked against a parameter fit of the Langmuir characteristic.[21,22] At low FEC gas pressure, Fig. 6 shows that the space potential in the FEC is strongly negative (−500 V) compared to that in the central cell. Ionization downstream of the double layer produces electrons which are accelerated back across the double layer in a monoenergetic beam. Our calculations indicate that the resultant Electron Velocity Distribution Function (EVDF) is unstable to the two-stream instability, suggesting that the instability is the source of the electrostatic oscillations.[23]

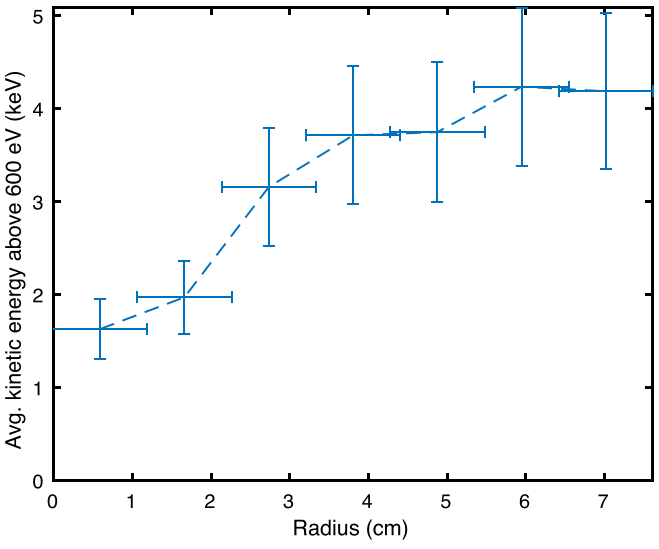

FIG. 7. The average electron kinetic energy for $E > 600$ eV, obtained by Abel inversion of deconvolved X-ray spectra as a function of radius.

As the FEC pressure increases, increased ionization in the FEC relaxes the current-free condition and the magnitude of the negative space potential decreases. This mechanism may also explain the findings in other experiments that the voltage drop over a current-free double layer sharply decreases at high downstream gas pressure.[24–27]

A phenomenon which may be important to the process of electron acceleration is the nonconservation of the magnetic moment of the electron, μ, in the PFRC-II. Large changes in μ in the mirror configuration, even in smooth fields, are well known.[28–32] Our simulations of electron trajectories confirm this behavior in the PFRC-II.[23]

We have considered a number of processes that could explain this electron energization and confinement. One is a novel model that joins two processes—μ nonconservation with Fermi acceleration due to the naturally occurring 200 MHz electrostatic fields near the nozzle magnet. The μ nonconservation allows longitudinal acceleration to overcome two supposed limitations: Causing the particle to enter the loss cone and the existence of Kolmogorov-Arnold-Moser (KAM) surfaces which limit particle acceleration.[33] This will be discussed in a future paper.

In summary, using X-ray spectroscopy, we have shown the existence of a multikilo-electron-volt electron tail in the central cell of a mirror machine whose plasma is sourced by a relatively low power capacitively coupled RF source outside the central cell. The effective temperature and the highest energies of these electrons exceed, by a factor of ten, those of the already high energies found near the plasma source.[6] These multikilo-electron-volt electrons strongly affect the space potential outside the central cell, but not in the central cell where their density is a small fraction of the bulk electrons.

We are grateful for the contributions of T. Qian, P. Jandovitz, and B. Berlinger. This work was supported, in part, by the Program in Plasma Science and Technology, DOE Contract No. DE-AC02-09CH11466, and IMOD Purchase Order No. 4440834795.

The digital data for this paper can be found at http://arks.princeton.edu/ark:/88435/dsp019s161896q.

REFERENCES

[1]J. H. Malmberg and C. B. Wharton, "Collisionless damping of large-amplitude plasma waves," Phys. Rev. Lett. **19**(14), 775–778 (1967).
[2]C. B. Wharton and J. H. Malmberg, "Microwave scattering from plasma waves," Phys. Fluids **11**(12), 2655–2664 (1968).
[3]M. Yamada, H. Ji, S. Hsu, T. Carter, R. Kulsrud, N. Bretz, F. Jobes, Y. Ono, and F. Perkins, "Study of driven magnetic reconnection in a laboratory plasma," Phys. Plasmas **4**(5), 1936–1944 (1997).
[4]M. A. Lieberman and A. J. Lichtenberg, *Principles of Plasma Discharges and Materials Processing* (John Wiley & Sons, 2005).
[5]K. Takahashi, H. Akahoshi, C. Charles, R. W. Boswell, and A. Ando, "High temperature electrons exhausted from RF plasma sources along a magnetic nozzle," Phys. Plasmas **24**(8), 084503 (2017).

[6]P. Jandovitz, C. Swanson, J. Matteucci, R. Oliver, J. Pearcy, and S. A. Cohen, "Demonstration of fast-electron populations in a low-pressure, low-power, magnetized RF plasma source," Phys. Plasmas **25**(3), 030702 (2018).
[7]I. Alexeff, G. E. Guest, D. Montgomery, R. V. Neidigh, and D. J. Rose, "Oscillations present in plasma-electron heating by an electron beam," Phys. Rev. Lett. **21**(6), 344–347 (1968).
[8]L. D. Smullin and W. D. Getty, "Generation of a hot, dense plasma by a collective beam-plasma interaction," Phys. Rev. Lett. **9**(1), 3–6 (1962).
[9]R. A. Demirkanov, A. F. Gevorkov, and A. F. Popov, "Plasma heating under beam instability conditions," in Plasma Physics and Controlled Nuclear Fusion Research. Proceedings of the Third International Conference on Plasma Physics and Controlled Nuclear Fusion Research, 1965.
[10]P. I. Blinov, L. P. Zakatov, A. G. Plakhov, R. V. Chikin, and V. V. Shapkin, "Plasma heating by an electric beam in a magnetic mirror machine," Sov. Phys. JETP **25**(3), 439 (1967).
[11]A. V. Arzhannikov, A. V. Burdakov, V. A. Kapitonov, V. S. Koidan, V. V. Konyukhov, S. V. Lebedev, K. I. Mekler, V. S. Nikolaev, V. V. Postupaev, D. D. Ryutov, M. A. Shcheglov, S. L. Sinitsky, S. G. Voropaev, and L. N. Vyacheslavov, "New experimental results on beam-plasma interaction in solenoids," Plasma Phys. Controlled Fusion **30**(11), 1571 (1988).
[12]J. E. Howard, A. J. Lichtenberg, M. A. Lieberman, and R. H. Cohen, "Four-dimensional mapping model for two-frequency electron cyclotron resonance heating," Phys. D: Nonlinear Phenom. **20**(2), 259–284 (1986).
[13]A. J. Lichtenberg, M. A. Lieberman, J. E. Howard, and R. H. Cohen, "Velocity diffusion in two frequency electron cyclotron resonance heating," Phys. Fluids **29**(4), 1061–1075 (1986).
[14]R. Bardet, P. Briand, L. Dupas, C. Gormezano, and G. Melin, "Hot-electron-plasma accumulation in the CIRCE mirror experiment," Nucl. Fusion **15**(5), 865 (1975).
[15]S. Cohen, "First operation of the PFRC-2 device," Bull. Am. Phys. Soc. **57**(12), 208 (2012).
[16]Amptek X-Ray Detectors and Electronics, http://amptek.com/ (last accessed January 1, 2018).
[17]C. Swanson, P. Jandovitz, and S. A. Cohen, "Using Poisson-regularized inversion of Bremsstrahlung emission to extract full electron energy distribution functions from x-ray pulse-height detector data," AIP Adv. **8**(2), 025222 (2018).
[18]T. M. O'Neil and J. H. Malmberg, "Transition of the dispersion roots from beam-type to Landau-type solutions," Phys. Fluids **11**(8), 1754–1760 (1968).
[19]W. E. Drummond, J. H. Malmberg, T. M. O'Neil, and J. R. Thompson, "Nonlinear development of the beam-plasma instability," Phys. Fluids **13**(9), 2422–2425 (1970).
[20]R. Schrittwieser, I. Axnas, T. Carpenter, and S. Torven, "Observation of double layers in a convergent magnetic field," IEEE Trans. Plasma Sci. **20**(6), 607–613 (1992).
[21]N. Hershkowitz, "How Langmuir probes work," *Plasma Diagnostics* (Elsevier, 1989), pp. 113–183.
[22]I. H. Hutchinson, *Principles of Plasma Diagnostics*, 2nd ed. (Cambridge University Press, Cambridge, MA, 2002).
[23]C. Swanson, "Measurement and characterization of fast electron creation, trapping, and acceleration in an RF-coupled, high-mirror-ratio magnetic mirror," Doctoral thesis (Princeton University, Princeton, New Jersey, USA, 2018).
[24]S. A. Cohen, N. S. Siefert, S. Stange, R. F. Boivin, E. E. Scime, and F. M. Levinton, "Ion acceleration in plasmas emerging from a helicon-heated magnetic-mirror device," Phys. Plasmas **10**(6), 2593–2598 (2003).
[25]C. Charles and R. Boswell, "Current-free double-layer formation in a high-density helicon discharge," Appl. Phys. Lett. **82**(9), 1356–1358 (2003).
[26]E. M. Aguirre, E. E. Scime, and T. N. Good, "Ion beams in multi-species plasmas," Phys. Plasmas **25**(4), 043507 (2018).
[27]X. Zhang, E. Aguirre, D. S. Thompson, J. McKee, M. Henriquez, and E. E. Scime, "Pressure dependence of an ion beam accelerating structure in an expanding helicon plasma," Phys. Plasmas **25**(2), 023503 (2018).
[28]L. R. Henrich, "Departure of particle orbits from the adiabatic approximation," in Proceedings of the Conference on Thermonuclear Reactions, United States Atomic Energy Commission, Gatlinburg, Tennessee, 1956.
[29]A. A. Garren, R. J. Riddell, L. Smith, G. Bing, J. E. Roberts, T. G. Northrop, and L. R. Henrich, "Individual particle motion and the effect of scattering in an axially symmetric magnetic field," J. Nucl. Energy (1954) **7**(3–4), 283–284 (1958).
[30]R. J. Hastie, G. D. Hobbs, and J. B. Taylor, "Non-adiabatic behaviour of particles in inhomogeneous magnetic fields," in Plasma Physics and Controlled Nuclear Fusion Research. Proceedings of the Third International Conference on Plasma Physics and Controlled Nuclear Fusion Research, Vol. I, 1969.
[31]R. H. Cohen, G. Rowlands, and J. H. Foote, "Nonadiabaticity in mirror machines," Phys. Fluids (1958–1988) **21**(4), 627–644 (1978).
[32]S. G. Tagare, "Motion of charged particles in an axisymmetric magnetic mirror," Phys. Rev. A **34**(2), 1587–1590 (1986).
[33]M. A. Lieberman and A. J. Lichtenberg, "Stochastic and adiabatic behavior of particles accelerated by periodic forces," Phys. Rev. A **5**(4), 1852–1866 (1972).